Normalisation of in-flight data

CB report No. 335

D.V. Bugg and A.V. Sarantsev

August 6, 1998

1 Abstract

This report presents details of the normalisation of in-flight data. The normalisation is derived from scaler data and the observed number of reconstructed events in each channel. Two independent studies have been made by David Bugg in QMWC and by Andrei Sarantsev in St. Petersburg. Their conclusions agree closely. The normalisation is well understood, but requires care in treating rate dependence.

The angular dependence of $d\sigma/d\Omega(\pi^0\pi^0)$ shows some small disagreement with results of Dulude et al. But the absolute normalisation of the cross section is much higher than theirs - by up to a factor 3. We conjecture that their normalisation may suffer from uncorrected technical problems with backgrounds of a similar nature to those we observe in Crystal Barrel.

2 Experimental Techniques

This report supercedes all previous information, much of which suffered from rate dependent effects which had not been fully understood.

2.1 The trigger

We are grateful to Willi Roethel for supplying the following summary. The trigger required is:
a) an incoming $\bar{p}$ defined by:

Si_C, the central silicon beam counter, in coincidence with Ken's chamber K, in anticoincidence with a 'High' signal in any of the four silicon quadrant counters,
in anticoincidence with either of the two veto scintillators,
b) an appropriate total energy signal from the barrel, above the threshold set in Tony's box,
c) zero-prong condition (according to Hartmut Kalinowski):
no hit in the Si-Vertex Detector,
no hit in JDC layers 2,3,9 and 10.

2.2 Monitoring the beam

We need to know the number of beam particles incident while the data-recording system was live. Unfortunately, this was not recorded directly - a pity, since it would have been so easy to do! Instead, the beam counter ran continuously, whether the data-handling system was live or dead. We monitor the livetime by means of three clocks, one of which appears to serve no useful purpose. One, C_1, ran continuously at 10 KHz; the second C_2 was inhibited when the data-handling system was dead and ran at 16 MHz. The third C_3 was like C_2 except that it ran at 1 MHz. It always agrees perfectly with C_2 within one count of the 16 MHz clock. Both of C_2 and C_3 were reset after every event, making it necessary to add up the gated scaler for every event on tape. The fractional live-time L is monitored from the sum of the gated clock, $\sum C_2$, divided by the ungated clock C_1:

$$L = \frac{\sum C_2}{1600 C_1}. \tag{1}$$

The number of beam particles incident while the system was live is then obtained by multiplying the beam scaler, $K.Si_C$, by the livetime: $N_B = K.Si_C.L$. This assumes that the spill is random. The spill was monitored frequently on the oscilloscope, where no structure to the beam was observed. A careful study of scaler ratios indicates no rate dependence over a wide range of intensities up to $4 \times 10^5 \bar{p}$/s. This shows that the livetime is monitored accurately.

$Triggers/K.S_C.L$ monitors the event rate per beam particle. Using the ratio of events fitted to any one channel (e.g. $\pi^0\pi^0$) per trigger, we compute the number of fitted events per beam particle; after correction for the reconstruction efficiency ϵ, this tells us the cross section, as described below.

Subsequent details come in two parts. The first part gives a mostly uninteresting summary of the things we have checked in our search to understand the normalisation and its reliability. The second part concerns conclusions about the normalisation and its systematic errors.

3 Part I. What we have monitored

The following ratios have been examined for every 1000 events throughout the entirety of the in-flight data. Most tell us little!

(i) $Si_{LU}/K.S_C$, $Si_{LD}/K.S_C$, $Si_{RU}/K.S_C$, $Si_{RD}/K.S_C$;
Si_C is the central beam defining silcon counter; the remaining Si are the four quadrants of the clover-leaf arrangement of silicon counters used for beam steering: left-upper, left-down, right-upper and right-down. Changes in the magnitudes of these ratios pinpoint occasions where the beam was being steered; uniformly high values of all four ratios indicate poor beam focussing. We use cuts on these four ratios to eliminate a few poor runs where the beam was badly mis-steered. We find that shapes of angular distributions and Dalitz plots are insensitive to beam conditions (steering, focussing, rate) within the available statistics. This implies that the kinematic fit is able to identify good events once a $\bar{p}$ interacts in the target. Our procedure in processing data is to keep as a sample of events ONLY events which fit at least one of the 42 hypotheses agreed between Bochum and the UK group with confidence level > 0.001. Following this we have fitted events kinematically to 4-8γ. (9 and 10γ events have been processed separately). We then fit events kinematically to 4-8γ, discarding all split-offs and merged pions. Let us denote by $N(n\gamma)$ the number of events kinematically fitted to $n\gamma$ with confidence level $> 10\%$; likewise we denote by $N(4-8)\gamma$ the total of $N(4\gamma)$ + $N(5\gamma)$ + $N(6\gamma)$ + $N(7\gamma)$ + $N(8\gamma)$. The ratio $N(4\gamma)/N(4-8)\gamma$ remains rock steady throughout a momentum, regardless of beam conditions. The same is true for the corresponding ratios for $5\gamma \ldots 8\gamma$. An illustration is provided in Fig. 1 for data at 1350 MeV/c. We display this momentum because high statistics data are available over a factor 2 range of intensities. What is plotted in (a) is the ratio $g4 = N(4\gamma)/N(4-8)\gamma$, i.e the ratio of events fitted kinematically with confidence level $> 10\%$ to 4γ compared with

the total of $4\gamma + 5\gamma + 6\gamma + 7\gamma + 8\gamma$ with the same confidence level. This plot is made for all events at 1350 MeV/c. In (b), the ratio $g6$ is shown for 6γ events and in (c) the ratio $g8$ for 8γ. In (d), the ratio is shown for $\pi^0\pi^0$ events. There is the merest hint of a decrease at low beam intensity. But other momenta show the merest hint of a rise instead, and when one views all momenta together, there is no evidence for rate dependence.

At other momenta, only a limited amount of data is available at low intensities, but again there is no evidence for any rate dependence of ratios; two examples are shown at 600 and 1800 MeV/c in Figs. 2 and 3.

So we have found no necessity to discard any runs for the purposes of calculating angular distributions, Dalitz plots, etc. This is a familiar story: measurement of absolutely normalised differential cross sections is MUCH harder than measuring the shape of the angular distribution.

In all this work, we have rejected split-offs and merged pions. As an alternative, we have evaluated results including split-offs using BRAIN. Ratios of cross sections again show no rate dependence, but ratios of cross sections are slightly different, because of the presence of cross-talk between channels.

(ii)$S_C/K.S_C$ and $K/K.S_C$;

these check the efficiencies of Ken's chamber and S_C. They also check for noise in S_C and K; no significant changes are observed, so these ratios are not very interesting.

(iii) $S_{OR}/K.S_C$; here S_{OR} is the sum of the four quadrant counters; it is sensitive to beam focussing.

(iv) $K.\bar{V}/K$ and $K.S_C.\bar{V}/K.S_C$;

the latter monitors the fraction of beam particles which interact in the target and the former the fraction of beam particles which interact in the target + S_C. If the beam were to miss a substantial fraction of the target, it would show up in these ratios, or if the target were to empty partially or completely; in practice, this does not happen.

(v) $K.S_C.L/C_1$;

this monitors beam intensity directly - the average number of beam counts per microsecond.

(vi) $Pile - up/Triggers$;

this monitors the fraction of events affected by pile-up and depends on beam rate.

All these quantities are formed from every 1000 events and displayed graphically. We have worked our way through all the runs in order to under-

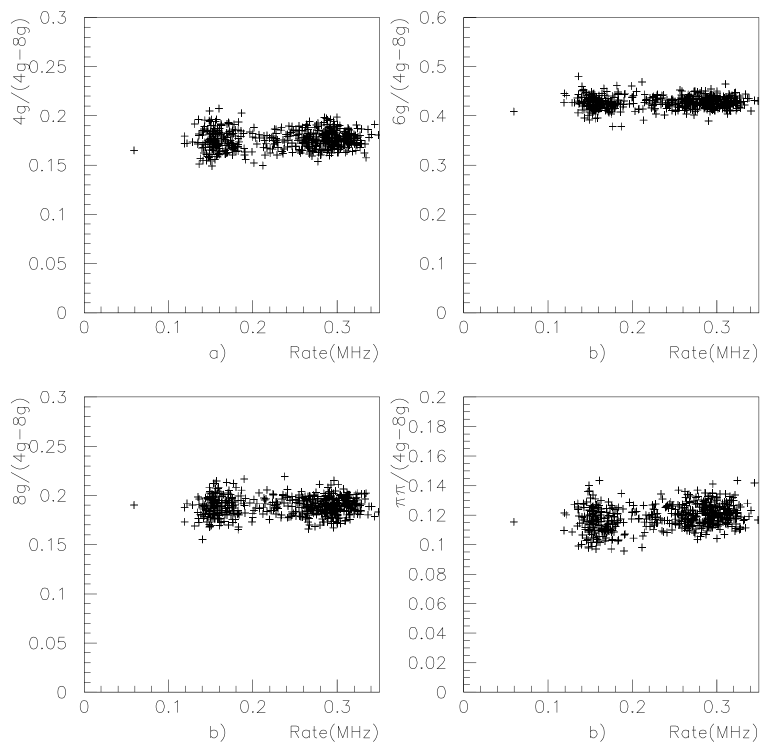

Figure 1: Ratios of fitted events (a) $N(4\gamma)/N(4-8)\gamma$, (b) $N(6\gamma)/N(4-8)\gamma$, (c) $N(8\gamma)/N(4-8)\gamma$, (d) $N(\pi^0\pi^0)/N(4-8)\gamma$ v. beam rate at 1350 MeV/c.

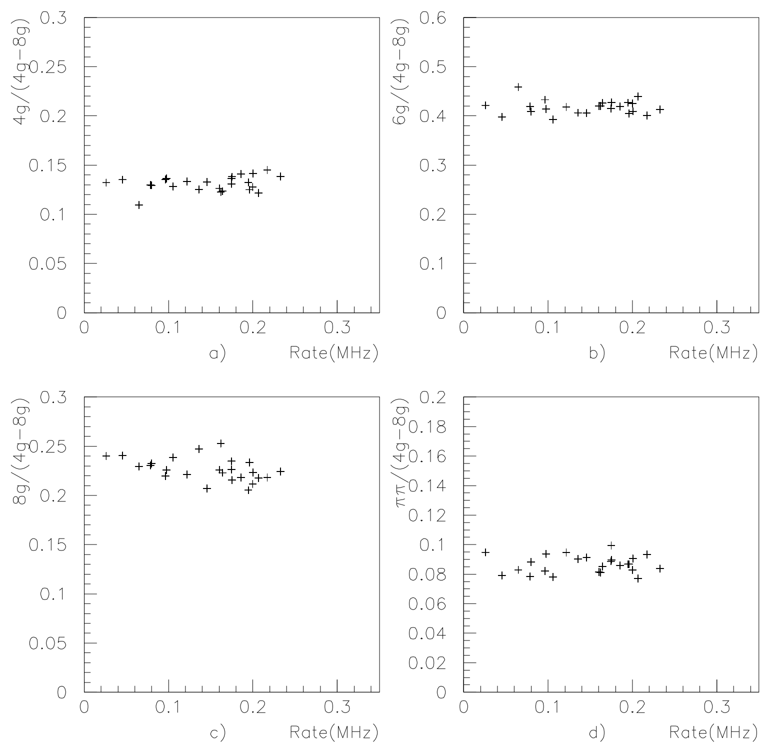

Figure 2: Ratios of fitted events (a) $N(4\gamma)/N(4-8)\gamma$, (b) $N(6\gamma)/N(4-8)\gamma$, (c) $N(8\gamma)/N(4-8)\gamma$, (d) $N(\pi^0\pi^0)/N(4-8)\gamma$ v. beam rate at 600 MeV/c.

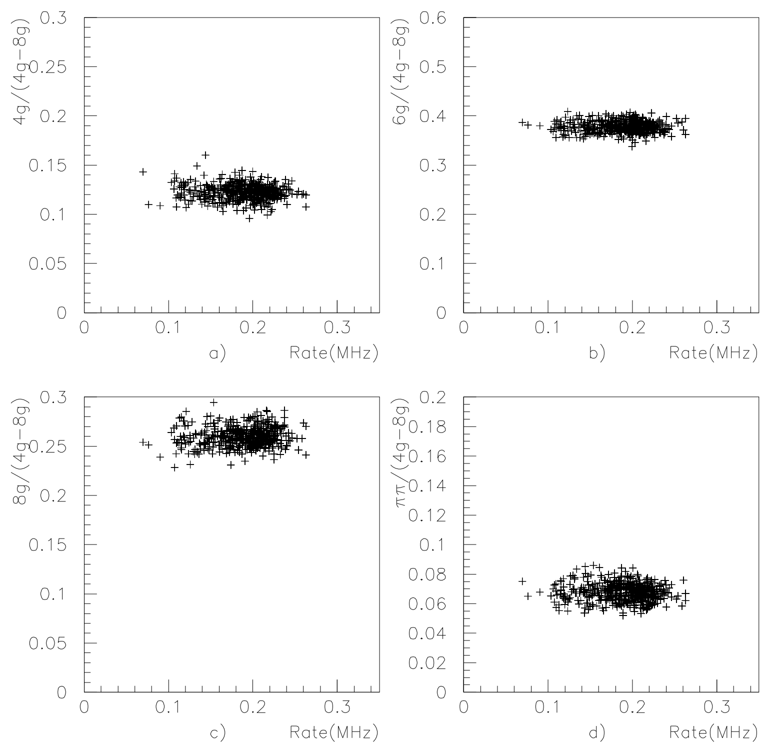

Figure 3: Ratios of fitted events (a) $N(4\gamma)/N(4-8)\gamma$, (b) $N(6\gamma)/N(4-8)\gamma$, (c) $N(8\gamma)/N(4-8)\gamma$, (d) $N(\pi^0\pi^0)/N(4-8)\gamma$ v. beam rate at 1800 MeV/c.

stand the factors which affect the normalisation. Eventually our conclusion is that the measured normalisation depends only on beam intensity and beam quality. Therefore the only scalers of interest for present purposes are those directly measuring cross sections and the beam rate and those monitoring beam focussing or steering, (i) and (iii).

4 Part II. The Normalisation

4.1 Principles

The basic idea is that one counts the incident beam particles, N_B, and uses the target length ℓ, the number of fitted events N_e in a particular channel ($\pi^0\pi^0$) and the Monte Carlo of the detector efficiency ϵ. The number of true events within solid angle Ω is $N_E = N_e/\epsilon$. Then the cross section is given by the well known relation:

$$\frac{N_E}{N_B} = N_{Av}\rho\ell \int_0^{\Omega} \frac{d\sigma}{d\Omega} d\Omega, \tag{2}$$

where N_{Av} is Avogadro's number and ρ is the density of liquid hydrogen (taken to be 0.070 gm/cm^3).

A small correction is needed for Dalitz pair production. The Monte Carlo generates only events of the variety $\pi^0 \to \gamma\gamma$. The probability that $\pi^0 \to \gamma e^+ e^-$ is 1.198%, and the probability that both $\pi^0 \to \gamma\gamma$ is $0.98798^2 = 0.97610$, so equn. (2) actually needs correcting upwards by 2.45%. We believe the Monte Carlo simulates all further effects, such as conversion of photons in the walls of the hydrogen target.

A possibility is that random vetoing by the veto counter could reject some genuine events. From tests during the run, this is believed to be negligible. The noise level of the veto was only a few counts per second with the beam off. From $K\bar{V}/K$, there is no evidence for rate dependence, hence no evidence for random vetoing.

4.2 Problems

We began by calculating cross sections from the elementary equn. (2). Results agreed closely with those of Willi Roethel - hardly surprising, since he made the same assumptions.

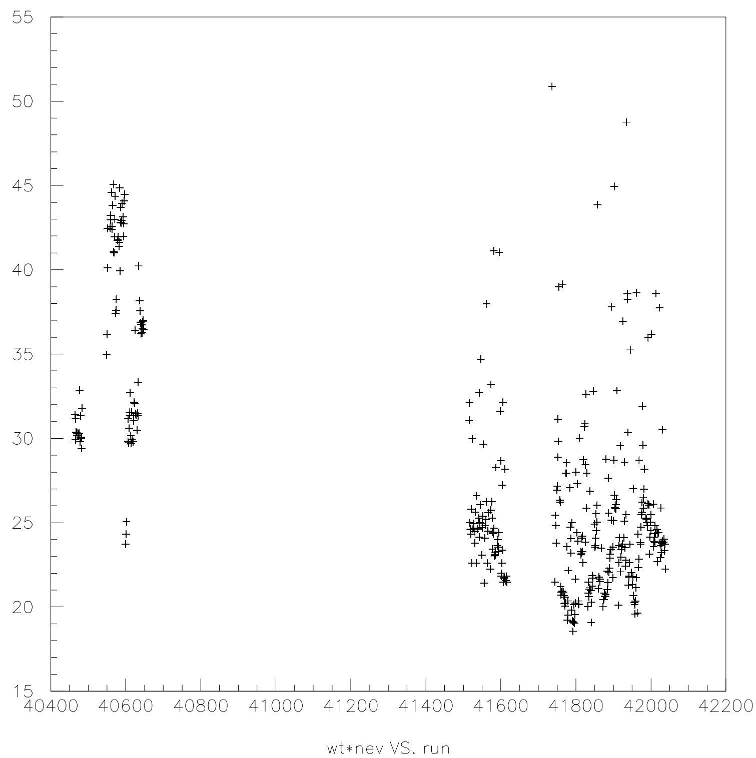

Figure 4: Normalisation (in arbitrary units) against run number.

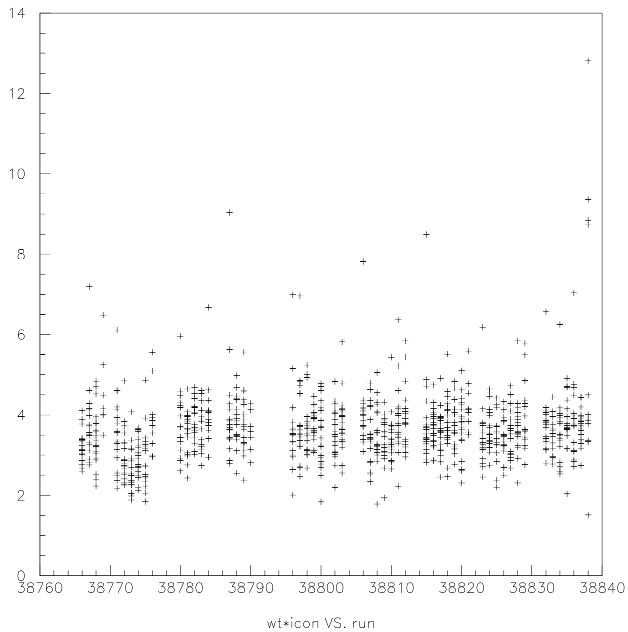

Figure 5: The normalisation of individual groups of 1000 events at the beginning of 1050 MeV/c data. High points are all at either the end or the beginning of the spill.

However, we noticed that there appear to be inconsistencies in normalisation between different groups of runs. This is illustrated in Fig. 4 for 900 MeV/c. The normalisation is plotted against run number in some arbitrary units which are not important for present purposes. For long periods of time, the normalisation remains steady, but then changes dramatically. Do not be alarmed! We later discovered the reason and after correction all the runs come into good agreement.

The clue to the problem lies in Fig. 5. The normalisation is plotted there for every 1000 events at the beginning of 1050 MeV/c. It immediately became clear that ALL the high points (above 6 with the scale shown there) lie at the beginning or end of a spill, where the beam rate is low. It reveals a VERY strong rate dependence of the normalisation. This rate dependence is easy to miss if one sums over a complete run. Each run is long enough that the average intensity is not too far from the average for the spill. The rate dependence arises not in the scalers, but in the fraction of events passing the kinematic fit. This shows a dramatic dependence on beam rate.

We determined the cross section from $N(4-8)\gamma$, the number of events fitting kinematically to $(4+5+6+7+8)\gamma$, for successive groups of 1000 events. Results are shown for four tapes at 1642 MeV/c in Fig. 6. Roughly 20% of events are reconstructed kinematically, so the statistical error on each cross in the figures is about 7%. What is plotted is a 'cross section' for $4\gamma - 8\gamma$, but WITHOUT correction for Monte Carlo efficiency of each event. That is, we have done the arithmetic on the number of fitted events in order to express the result in microbarns, using equn. (2). Our hope is that this can serve as a reference number for the analysis of further channels. When anyone analyses a particular channel, he or she can use these numbers to obtain an absolute normalisation simply by using the ratio of events in that channel compared with the full sample of $4-8\gamma$ events.

On Fig. 6, there is a very strong, but approximately linear dependence of normalisation on beam intensity. The blobs in every panel are taken at high intensity in the middle of each spill. The discrepancies in rate between the panels are responsible for the shifts observed in Fig. 4. Only the events at the very end or very beginning of each spill are at a low enough intensity to determine the extrapolation to zero rate. (It is a crying shame that the full tests we requested at 1/10 normal beam intensity were not made). The lines on Fig. 6 have been fitted separately to each tape, in order to estimate the uncertainty in the extrapolation.

Fig. 7 shows results at (a) 1800, (b) 1525, (c) 1350 and (d) 1050 MeV/c. Figs. 8(a) and (c) show results at 900 and 600 MeV/c respectively. There, the rate dependence is very large, and it becomes clear that the dependence on rate is non-linear. We have therefore made the extrapolation to zero rate using only the events at the lowest rates. These are displayed in Figs. 8(b) and (d). The curvature can just be discerned at 1050 MeV/c too, but becomes invisible for higher momenta.

The pile-up flag does not help in getting rid of the rate dependence. Even at high intensities, the pile-up flag is set only 1% of the time. If one rejects events with the pile-up flag set, there is hardly any visible change in

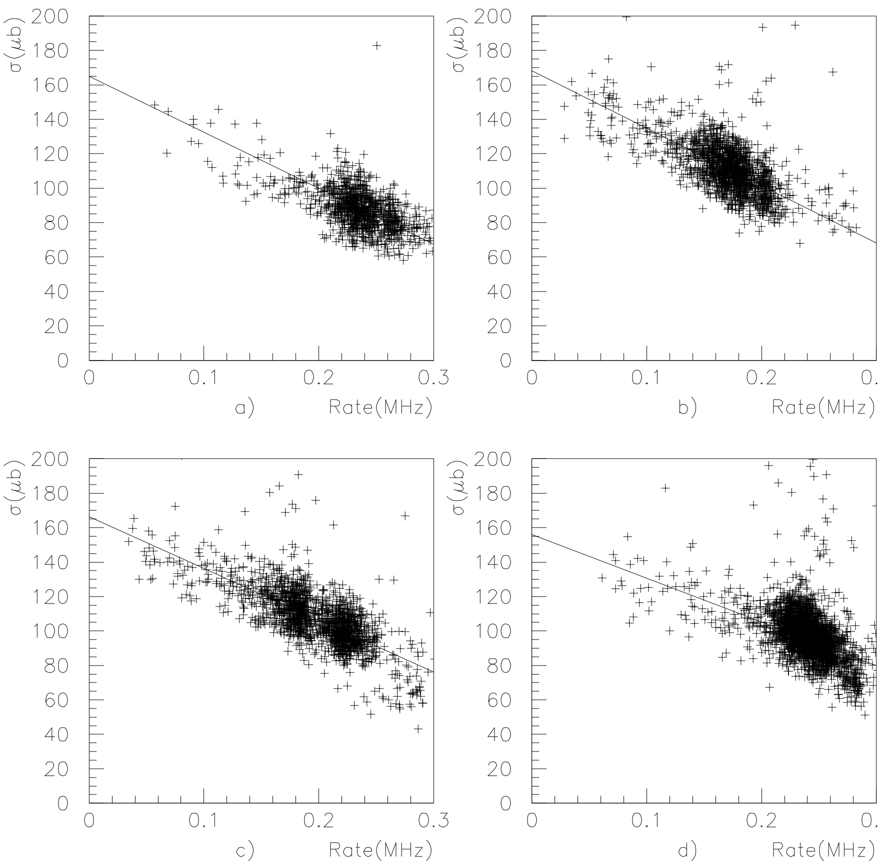

Figure 6: Dependence of $'\sigma(4-8)\gamma'$ on beam intensity for four tapes at 1642 MeV/c; here σ is UNCORRECTED for Monte Carlo efficiency.

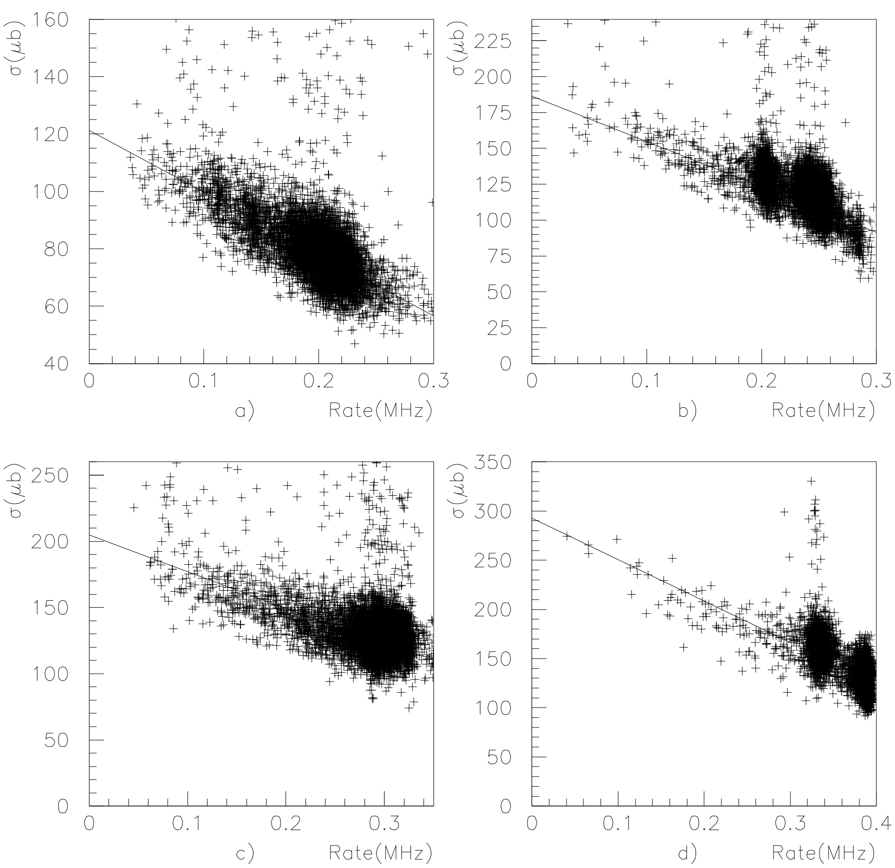

Figure 7: As Fig. 6 at (a) 1800, (b) 1525, (c) 1350 and (d) 1050 MeV/c.

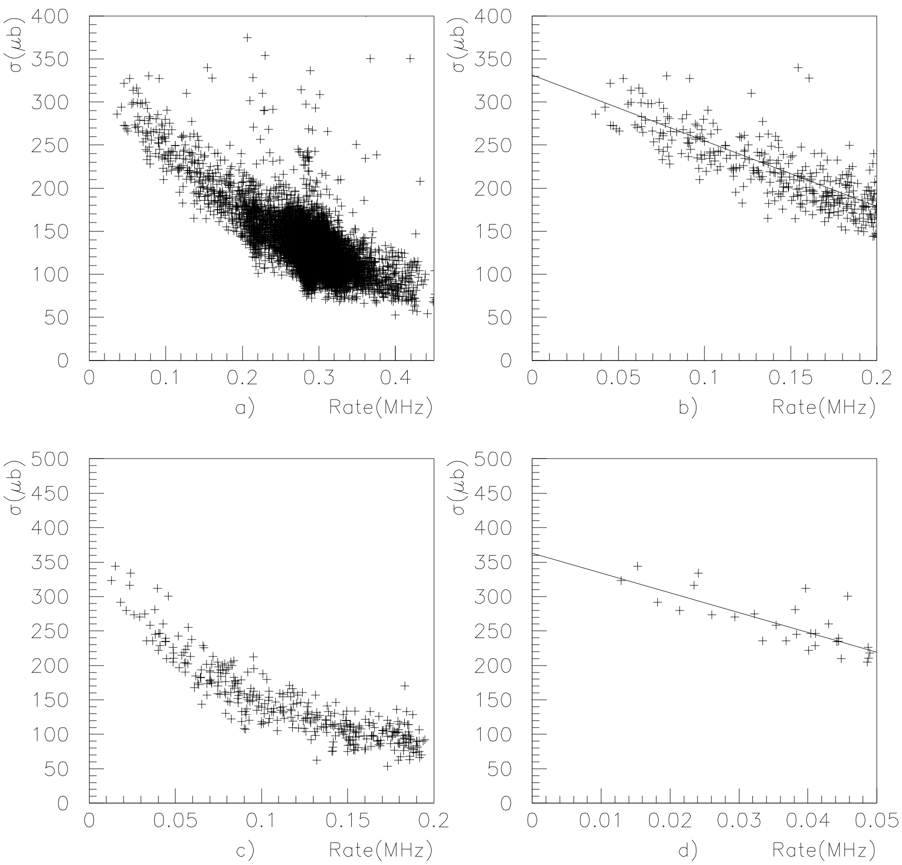

Figure 8: (a) As Fig. 6 at 900 MeV/c; (b) a blown-up view of (a) at the lowest beam rates; (c) and (d) ditto at 600 MeV/c.

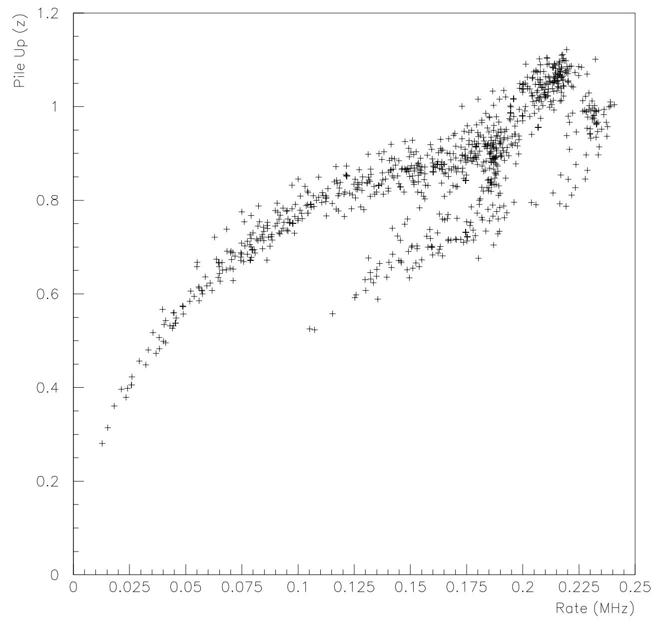

Figure 9: Percentage of events at 600 MeV/c for which the pile-up flag is set, as a function of beam intensity.

the observed rate dependence. It is obvious that the pile-up flag is actually monitoring $\leq 2\%$ of the actual pile-up. Perhaps the pile-up flag was not operating correctly. Its dependence on rate is shown for one momentum in Fig. 9. We have been unable to make any sense out of this dependence. However, there appears to be little uncertainty from Figs. 6–8 in making the extrapolation to zero rate. And from Figs. 1-3, branching ratios between channels are accurately independent of rate.

5 How does the rate dependence originate?

The rate dependence is worst at 600 MeV/c, despite the use of modest beam intensity. So we inspected the 600 MeV/c data. The total energy spectrum is displayed for several runs in Fig. 10. A peak is clearly visible corresponding to the full energy of a $\bar{p}p$ interaction, ~ 2000 MeV. What we find is that runs with high backgrounds under the total energy peak give low normalisation. The background increases non-linearly with intensity, but also depends on beam quality. The decrease in normalisation is directly related to the background level. At higher momenta, the backgrounds under the total energy peak are lower but still present. Examples are shown in Fig. 11.

The alarming feature of the total energy spectrum is that there are events present with substantially MORE energy than should be available from a $\bar{p}$ of the beam energy interacting with a proton. Interactions of a $\bar{p}$ with a nucleus cannot generate substantially more energy, so that does not offer an explanation. The PEDs tend to cluster around the downstream beam hole. This is illustrated in Fig. 12, which shows the angular distribution of the PEDs (in the lab). The full histogram shows the angular distribution for events in the full energy peak; the dashed histogram shows the angular distribution for events with energies $>$ 400 MeV above the full energy peak. Secondly, one frequently finds a large bunch of peds with similar θ (polar angle) and ϕ (azimuth).

We have selected events with energies at least 400 MeV above the total energy peak and compared them with events in the total energy peak. There is a dramatic difference. For the former, even with an energy 400 MeV above the total energy peak, the average number of peds is 14.1, compared with 7.5 for the total energy peak. What is happening is that events with large background, hence large multiplicity, fail to reconstruct kinematically. The background kills genuine events. This effect is not simulated by the Monte Carlo. Our interpretation of the background is that it arises from $\bar{p}$ which miss S_C and annihilate in the downstream part of the barrel, producing pile-up on top of normal events. The effect is severe at low momenta for two possible reasons: (a) increased multiple scattering in material upstream of the target, (b) a wider diffraction pattern for $\bar{p}p$ or $\bar{p}-$Nucleus elastic scattering. Somebody should inspect the gas data at rest for a corresponding effect; the background under the total energy increases drops rapidly with decreasing beam momentum.

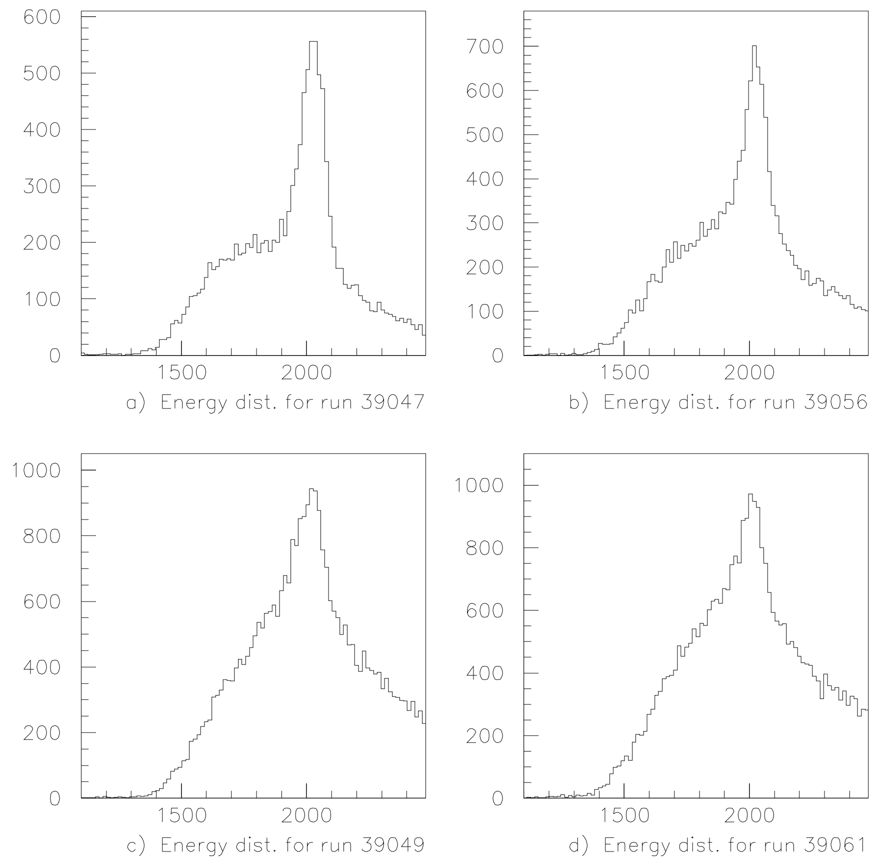

Figure 10: The total energy spectrum for progressively higher beam intensities (a) $\rightarrow$ (d) at 600 MeV/c.

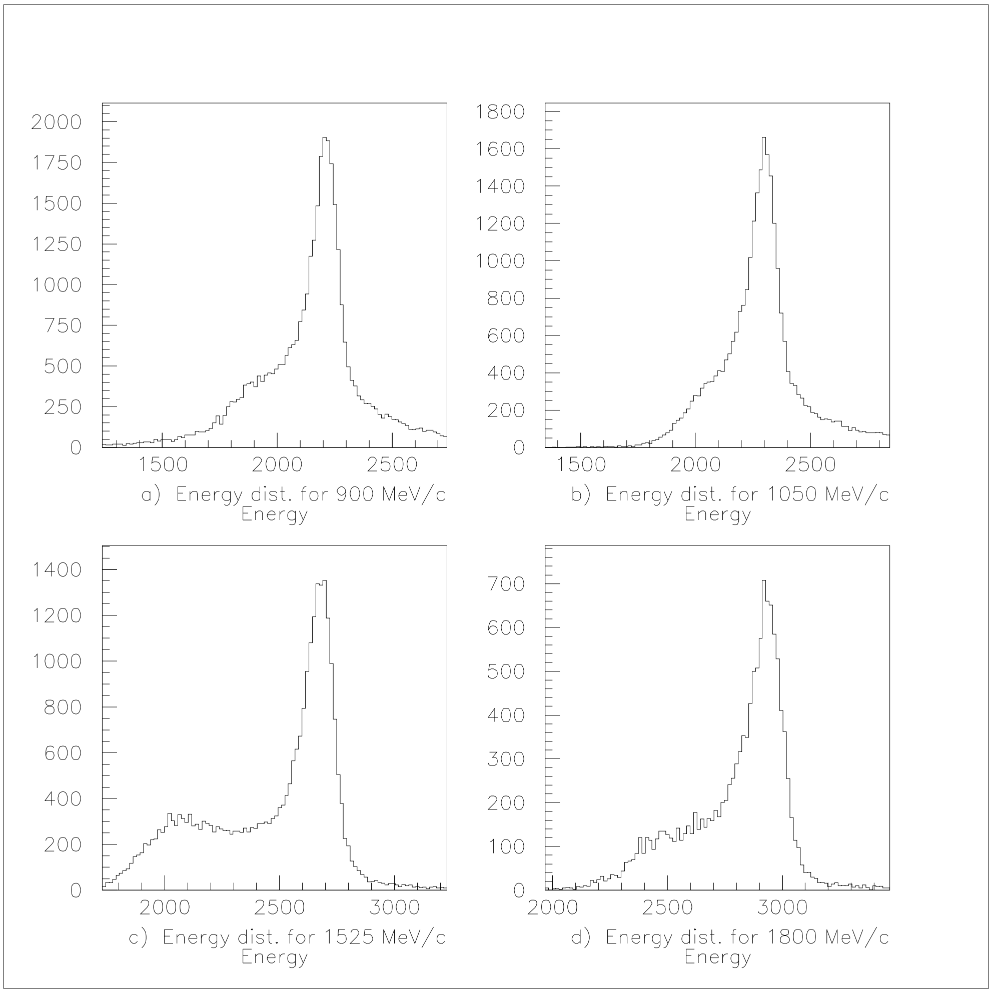

Figure 11: The total energy spectrum at (a) 900, (b) 1050, (c) 1525 and (d) 1800 MeV/c.

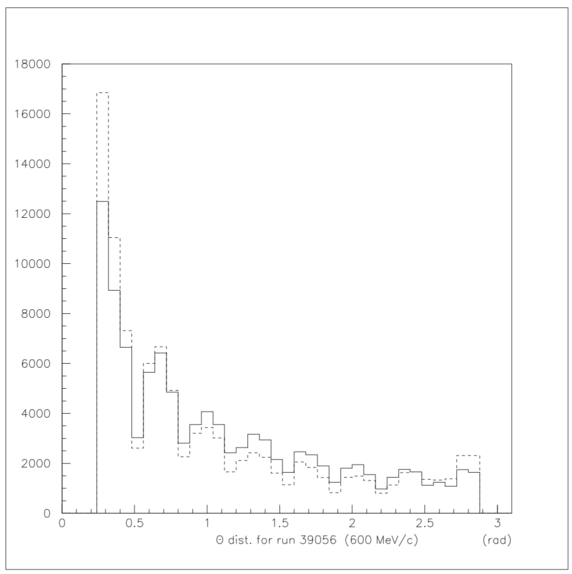

Figure 12: Angular distributions of PEDs; the full histogram is for events in the full energy peak and the dashed histogram is for events with total energy > 400 MeV above the full energy peak.

Most likely, background originates from events where beam particles miss Si_C. Background events out of time with a genuine events are not vetoed in the trigger logic. Most of the data were taken at an intensity of $(2-4)\times 10^5$ $\bar{p}$/s. With a 6μs recovery time for the shapers, one would get 50% background if $\sim$ 27% of the beam misses Si_C and annihilates in the barrel. However, this argument assumes perfect functioning of the shapers. Part of the CsI pulse has a 100μs decay time, which is supposed to be eliminated by pole-zero cancellation in the electronics, leaving a pulse with 6μs time constant. However, this electronic correction may not be perfect. It is possible that significant pile-up persists for $> 100\mu$s, particularly in crystals near the beam exit, where event rates are high.

We have observed that the slope of the rate dependence changes with beam conditions. At 900 MeV/c, one batch of data was taken in August 1996 and a second in October. The rate dependence has a significantly different slope, but results extrapolate to the same normalisation at zero beam rate. This is illustrated in Fig. 13 for four very different sets of beam conditions. Figs. 13(a) and (b) were taken from the August run, when the beam was well focussed. The change between (a) and (b) occurred at a point where the logbook says that beam sharing with another user was set up. Figs. 13 (c) and (d) were taken from the October run. In that run, the beam was deliberately defocussed to some extent, to reduce the observed radiation damage to S_C. This defocussing increased the background under the total energy peak quite strongly. The October data show a distinctly non-linear extrapolation which is evident in Fig. 8(a). Therefore in Figs. 13 (c) and (d) , we display only data below a rate of 0.2 MHz. The straight lines on the figures extrapolated to 0.4 MHz give values of 180, 90, 40 and 20 resepectively, demonstrating the difference in slopes. The lines have all been drawn through the same cross section, 330 μb at zero rate. You can use your own judgement to assess the variation which might be present between these four very different beam conditions. We reckon a $\pm 6\%$ error covers it.

Fig. 14 shows two extrapolations under very different beam conditions at 1050 MeV/c. Although the slopes of the extrapolations differ by about 30%, there is no significant difference in the cross section extrapolated to zero rate.

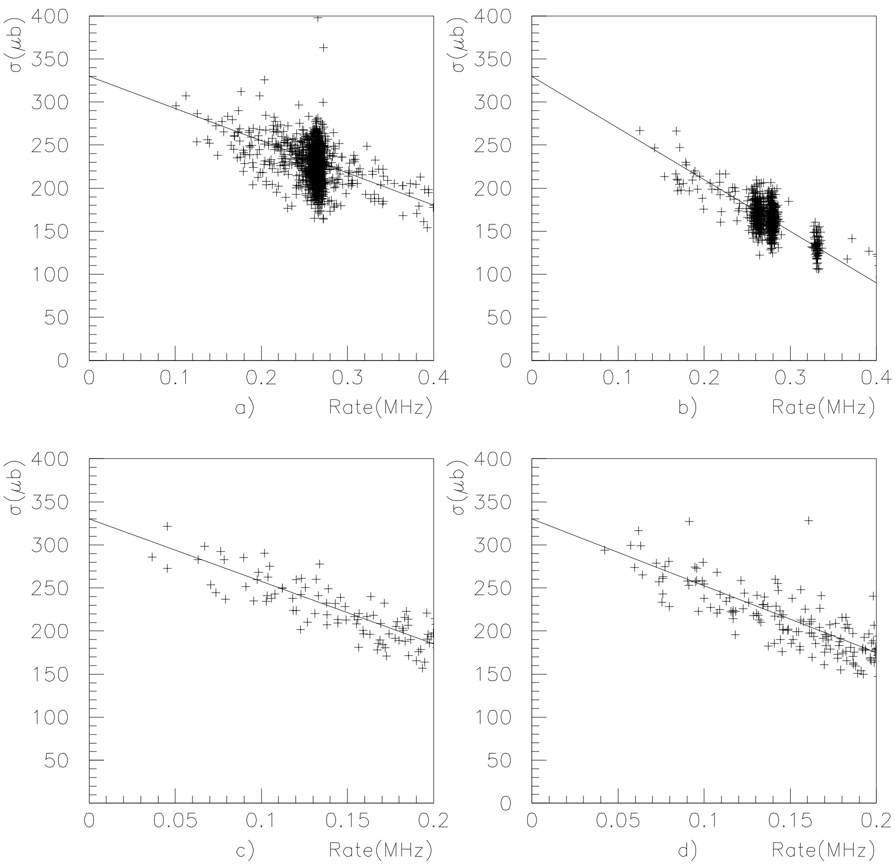

Figure 13: The extrapolation to zero rate for four very different beam conditions at 900 MeV/c, as described in the text.

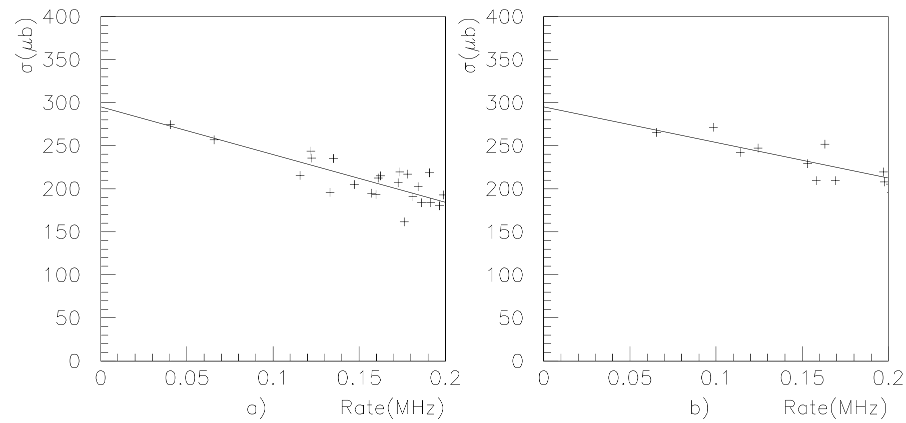

Figure 14: The extrapolation to zero rate at 1050 MeV/c under very different beam conditions.

5.1 Detailed recommendations on choice of runs

1) It is ESSENTIAL to determine the normalisation using groups of events as small as 1000 in order to get the best information on the extrapolation to zero rate. DO NOT average over complete runs. If you do, you throw away the crucial samples at the lowest beam intensities.

2) For 1050 MeV/c, determine the absolute normalisation only from tapes GK0485 and GK0486. The three remaining tapes have a threshold on Tony's box which is set dangerously high, and there is a visible effect on branching ratios. However, as far as we can tell, this has no effect on angular distributions or Dalitz plots, for which these tapes can be used safely.

3) At 1350 MeV/c, tapes GKO490 and GK0491 contain ONLY data at high intensity. There is no discrepancy between these and other tapes as regards branching ratios, but they should not be used for the extrapolation to zero rate.

4) The same is true at 600 MeV/c for runs 39071 upwards.

5) We choose, for simplicity, to reject all runs with < 2000 events, since these usually are subject to some trivial error by people on shift.

6) Otherwise, all tapes can be used without problems.

6 The summed cross sections

Fig. 15 shows the summed cross section (above 10% confidence level) for events fitting 4 or 5 or 6 or 7 or 8 γ. Let us call this $'\sigma(4-8)\gamma'$. It varies nearly linearly with beam momentum, as shown by the straight line. But 1350 MeV/c is a little low compared with other points. Is this real or not? We think it is. There are probably small enhancements around 900 and 1750 MeV/c, where Zou's analysis of $\eta\pi^0\pi^0$ data (and Ryabchikov's analysis of VES data) reveals towers of resonances (masses $\sim$ 2040 and 2330 MeV). Fig. 16, for the 1350 MeV/c data illustrates two points. Firstly, it has been evaluated from complete runs, rather than from groups of 1000 events as in Fig. 7(c). This grouping cleans up the appearance of the plot greatly compared to Fig. 7(c), because of the higher statistics in complete runs. The same extrapolation is shown there as in Fig. 7(c) by the full line. However, we believe it is more accurate to evaluate the cross section from Fig. 7(c), because points extend to lower rates than in Fig. 16. The dashed line is

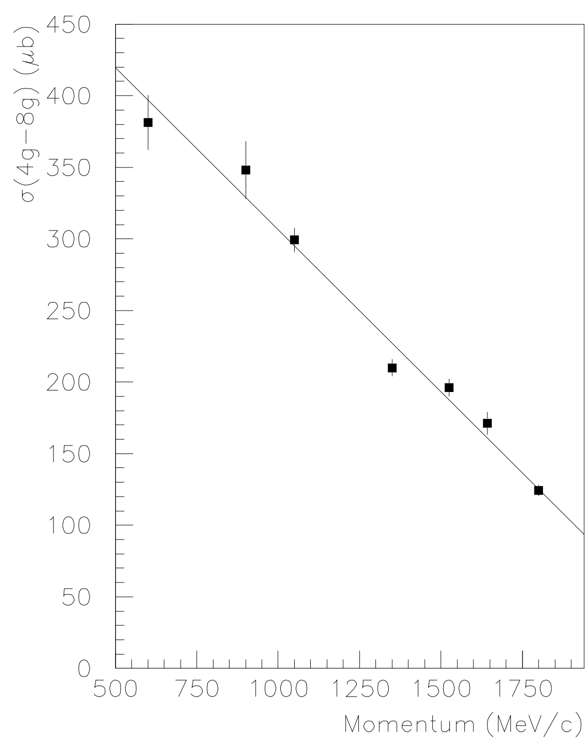

Figure 15: $'\sigma(4-8)\gamma'$ v. momentum, UNCORRECTED for Monte Carlo reconstruction efficiency. The straight line is fitted by eye.

drawn for $'\sigma(4-8)\gamma'$ taken from the straight line drawn on Fig. 15, i.e. 230 μb. It is obvious by eye that the dashed line on Fig. 16 extrapolates to a value which is too high. The difference in extrapolated cross section between dashed and full lines is 12%.

We have estimated the error in the extrapolation to zero rate by fitting many groups of runs, and also by assessing by eye what is visibly a poor fit. The error varies from 3% at high momenta to 6% at 900 MeV/c. There could be a further small systematic error of $\sim 3\%$ from our assumption of a linear extrapolation at low rates; but we are confident that this systematic error varies slowly with momentum. It could, for example, change from 3% at 600 MeV/c to 0 at 1800 MeV/c or vice versa. Such a slow variation is irrelevant in looking for $s-$channel resonances, our primary objective. Crystal Barrel techniques cannot be claimed to give better than 6–8% absolute normalisation overall, bearing in mind possible errors in target length and density.

7 Results and comparison with Dulude et al.

Our acceptance, ϵ, for $\pi^0\pi^0$ events as a function of $\cos\theta$ (the production angle in the centre of mass system) is shown by the dashed curve in Fig. 17 at 1350 MeV/c. It is very similar at other momenta. It is derived from the Monte Carlo simulation. It drops sharply for $|\cos\theta| > 0.85$. Our measured $\pi^0\pi^0$ events are corrected by dividing by ϵ over the range up to $\cos\theta = 0.85$. Thus, in comparing with Dulude et al. [1], we have used their differential cross sections integrated over this range of $\cos\theta$. The procedure for obtaining the absolutely normalised cross section is as follows:

$$Measured\ \sigma = 2\pi \int_0^{0.85} \frac{d\sigma}{d(\cos\theta)} \epsilon(\cos\theta)\ d(\cos\theta), \tag{3}$$

$$True\ \sigma = 2\pi \int_0^{0.85} \frac{d\sigma}{d(\cos\theta)}\ d(\cos\theta). \tag{4}$$

For any particular $\cos\theta$, the measured differential cross section is

$$[\frac{d\sigma}{d\Omega}(\cos\theta)\epsilon(\cos\theta)].$$

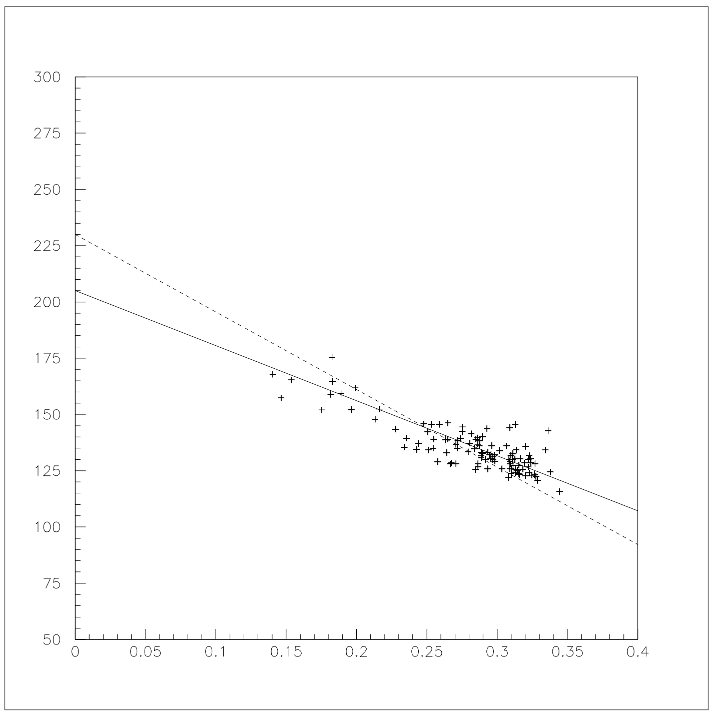

Figure 16: The rate dependence of $'\sigma(4-8)\gamma'$ at 1350 MeV/c, but extrapolated to 230 μb (on the straight line of Fig. 15).

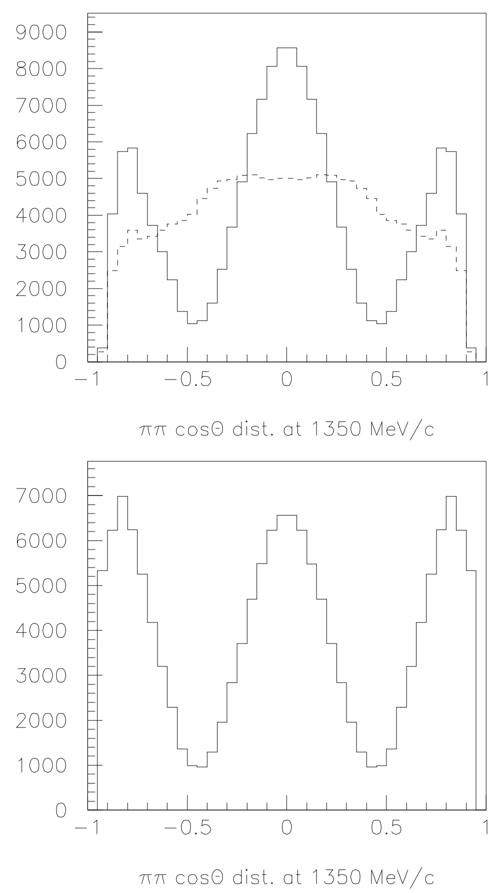

Figure 17: Angular distribution at 1350 MeV/c for $\pi^0\pi^0$. The upper figure shows the measured angular distribution before acceptance correction as a histogram; the acceptance is shown by the dashed curve. The lower figure shows the angular distribution after the acceptance correction.

Hence we compute the integrated cross section $\sigma_{\pi\pi}$ as

$$\sigma_{\pi\pi} = 2\pi \int_0^{0.85} \frac{\frac{d\sigma}{d(\cos\theta)}\epsilon(\cos\theta)}{\epsilon(\cos\theta)}\, d(\cos\theta). \tag{5}$$

The integration is over only one hemisphere - i.e. each $\pi^0\pi^0$ event is counted only once.

Table 1 lists $'\sigma(4-8\gamma)'$ and $'\sigma(\pi^0\pi^0)'$ UNCORRECTED for Monte Carlo efficiency; the last column shows the true $\sigma(\pi^0\pi^0)$ AFTER correction for efficiency according to the preceding equations. There are some very minor differences between $'\sigma(4-8\gamma)'$ of Table 1 and the extrapolations shown in Figs. 6-8. This is because ALL runs have been used for Table 1, while in Fig. 6-8 some tapes with different beam conditions (hence different extrapolations) are omitted, so as to keep the figures clear.

Results for the integrated cross section are shown in Fig. 18 for $\pi^0\pi^0$. There are major disagreements with Dulude et al. [1]. Their angular distributions agree at some momenta, but not all, within their rather large error corridors after scaling their normalisation to agree with ours; Fig. 19 illustrates one momentum where there is agreement and one momentum where there is some disagreement. Willy Roethel has found agreement from the fine-scan data. We conjecture that results of Dulude et al. may suffer from a pile-up problem of the same variety as we have observed. They used a partially separated beam of $\bar{p}$ contaminated by π^-. They do not quote the rate they used, nor do they mention tests for rate dependence. It is plausible that $\bar{p}p$ annihilations and π^-p charge exchange may have generated backgrounds which caused them to discard events. We have discussed possible sources of error with David Peaslee, who is a personal friend and was a member of the Dulude et al. experiment. These discussions have failed to locate the source of the discrepancy.

We do not compare with Hasan and Bugg [2], since that analysis incorporated the Dulude et al. data. In principle, $\pi^-\pi^+$ data allow a separation of $I=0$ and $I=1$ components of the cross section from a forward-backward asymmetry which depends on the interference between them. In practice, $I=0$ and $I=1$ amplitudes are found to be closely orthogonal, and the interference is too small to separate $I=0$ and $I=1$ cross sections reliably. If one looks at the raw data, the angular distributions have an approximate forward-backward symmetry.

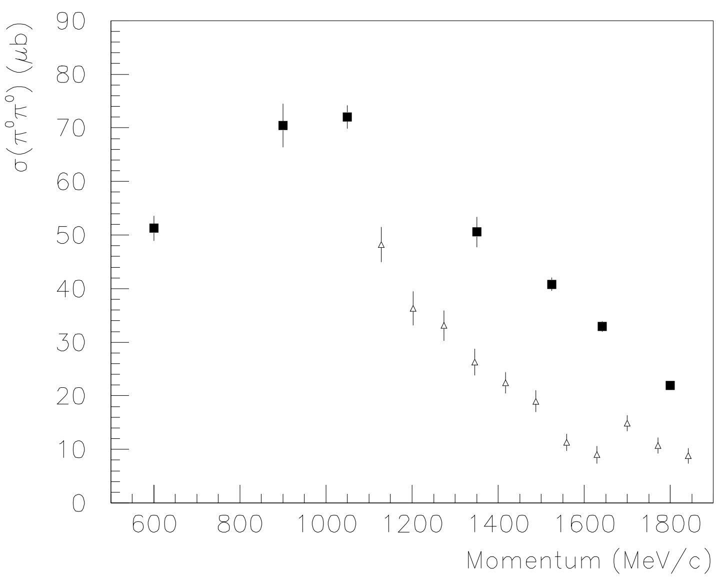

Figure 18: $\sigma(\pi^0\pi^0)$ integrated over the range of $\cos\theta$ zero to 0.85. Black squares are Crystal Barrel results and open triangles those of Dulude et al.

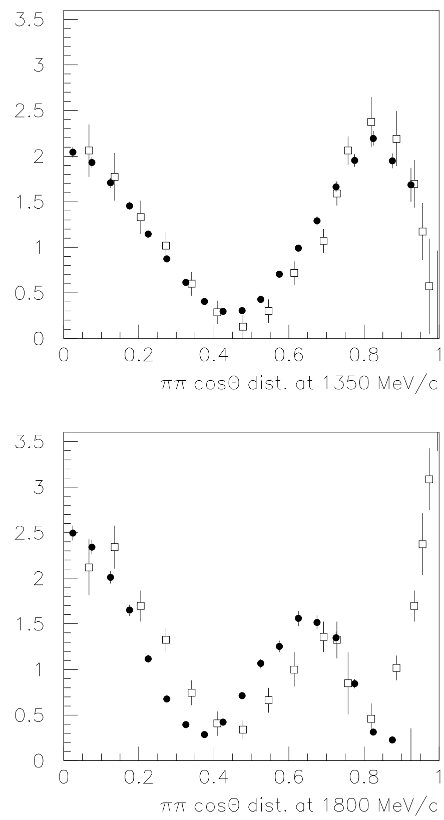

Figure 19: Comparison of $d\sigma/d\Omega(\pi^0\pi^0)$ from Crystal Barrel (black points) and Dulude et al, (open squares) at two mo menta close to ours: (a) our 1350 MeV/c compared with their 1361 MeV/c, (b) our 1800 MeV/c compared with their 1799 MeV/c.

8 How could our normalisation be wrong?

We are confident of our normalisation after the correction for rate dependence. We see no realistic possibility of cross-checks from other processes, e.g $\bar{p}p \to \pi^-\pi^+$, because of the problem of assessing split-offs from charged tracks accurately; this is known from Nana's work to have large systematic errors, of the order of a factor 2.

So we now consider what further errors might be present in the present determination.

(A) The beam counts could be wrong through failure of the scaler. But if so, there is no evidence for changes with time or beam momentum. It seems implausible that a faulty scaler would misbehave so reliably! However, our principle concern is with the *relative* normalisation between momenta, and that appears reliable.

(B) It hardly seems likely that the target length or density is wrong by a large factor. If the target were to contain a gas bubble, this would fluctuate with time over a run approaching 4 months. The effect of the curved end of the target for large beam size at 600 MeV/c is at most a 2% correction, and that is smaller than the present systematic uncertainty.

(C) Is the Monte Carlo esimate of acceptance reliable? Past experience is that closely similar results are obtained for $\eta \to \gamma\gamma$ and $\eta \to 3\pi^0$ in (i) 4γ and 8γ events and from 6γ and 10γ events. We have made our own comparison for $\eta\eta$ and $\pi^0\eta$ and results will be presented in a later technical report on those data. There is excellent agreement, well within the errors, so it looks unlikely that the Monte Carlo is seriously in error.

(D) We have evaluated $d\sigma/d\Omega(\pi^0\pi^0)$ for confidence level cuts of 1% and 20%. Results in Fig. 20 agree within statistics, showing that the precise confidence level at which events are selected is not critical. Incidentally, there has been discussion within the collaboration of the precise calibration of high energy photons. The forward differential cross section at high momenta is sensitive to that calibration. Fig. 18 demonstrates that uncertainties in the calibration have an effect smaller than statistics.

(E) As a further test, we have evaluated $d\sigma/d\Omega(\pi^0\pi^0)$ at several momenta for groups of runs with beam intensities varying by a factor 2. There is no significant change in the shape of the angular distribution. An example is shown in Fig. 21 at 1350 MeV/c. One set of points is shown by error bars and the other by squares which indicate the errors. One set of data was taken

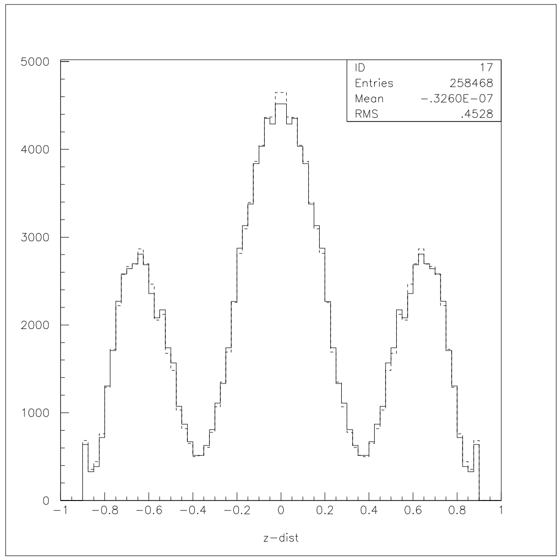

Figure 20: $d\sigma/d\Omega$ at 1525 MeV/c with 1% confidence level cut (full histogram) or 20% confidence level cut (dashed histogram).

at a mean rate of 150 KHz and the other at over 300 KHz.

9 Cross Section Ratios

Table 2 shows ratios of reconstructed 4γ, 6γ and 8γ events to $'\sigma(4-8)\gamma'$, WITHOUT any correction for Monte Carlo efficiency. The last column shows the corresponding ratio for $\pi^0\pi^0$. It is our hope that these ratios, taken together with Table 1, may offer a convenient means of normalising other channels.

10 Normalising earlier runs

The value of $'\sigma(4-8)\gamma'$ is obtained at 1200 MeV/c as the average of results at 1050 and 1350 MeV/c; that at 1940 MeV/c is obtained from the straight

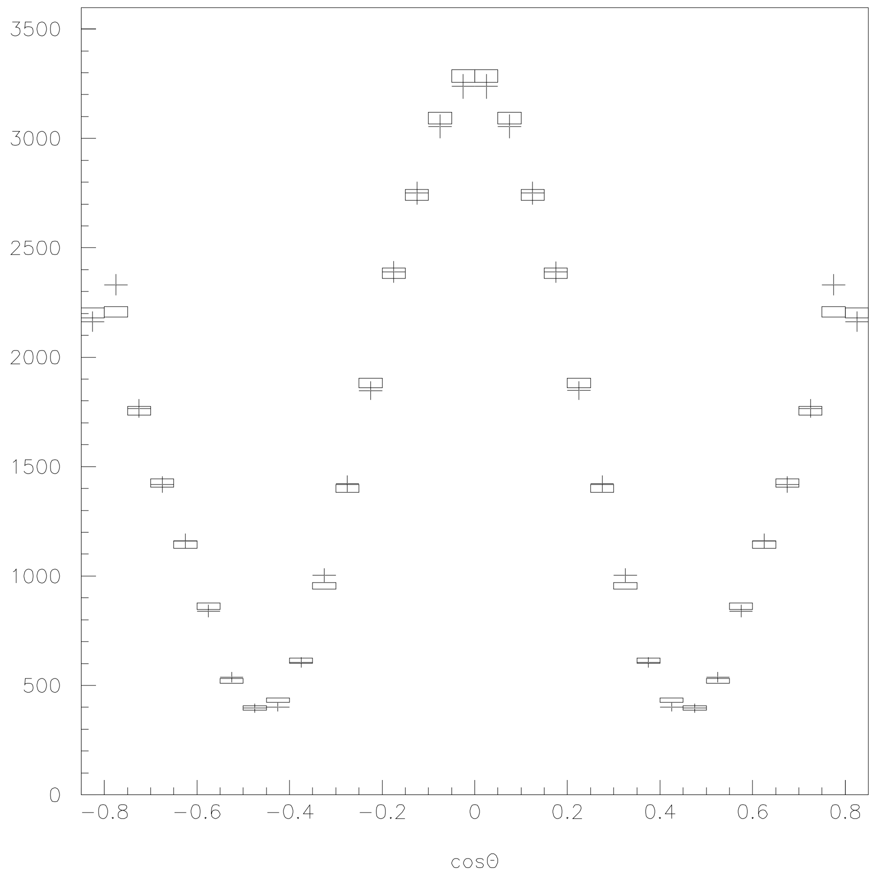

Figure 21: $d\sigma/d\Omega$ at 1350 MeV/c with 10% confidence level cut at intensities of 150 KHz (shown by points with errors) and 325 KHz (shown by open squares whose size indicates the errors).

line of Fig. 13. Then the ratio of 4γ to $(4+5+6+7+8)\gamma$ is obtained from the data themselves at those momenta; They are shown in Table 2. This then allows us to normalise the $\pi^0\pi^0$ data at 1200 and 1940 MeV/c. We choose to interpolate in $'\sigma(4-8)\gamma'$ because it shows vastly smaller momentum dependence than individual channels like $\pi^0\pi^0$.

11 Conclusion

Our results pass all of the tests we have been able to devise. The rate dependence is large and it is ESSENTIAL to carry out the extrapolation to zero beam rate. Our conclusion is that the absolute normalisation of Dulude et al. is simply wrong.

References

[1] R.S. Dulude et al., Phys. Lett. 79B (1978) 329 and 335.

[2] A. Hasan and D. Bugg, Phys. Lett. B334 (1994) 215.

[3] E. Eisenhandler et al., Nucl. Phys. 113B (1976) 1.

Momentum (MeV/c)	$'\sigma(4-8)\gamma'(\mu b)$	$'\sigma(\pi^0\pi^0)'(\mu b)$	$\sigma(\pi^0\pi^0)(\mu b)$
600	372.0 ± 19.1	34.0	51.3 ± 2.3
900	339.6 ± 20.2	44.2	70.4 ± 4.1
1050	291.9 ± 8.4	44.6	72.0 ± 2.2
1200	248.5 ± 10.8	34.1	65.3 ± 2.8
1350	205.1 ± 8.8	25.4	50.6 ± 2.8
1525	191.4 ± 6.1	18.5	40.8 ± 1.2
1642	167.2 ± 7.9	13.9	33.0 ± 1.0
1800	122.3 ± 4.0	8.4	22.0 ± 0.7
1940	93.55 ± 9.4	5.9	17.8 ± 1.8

Table 1: Measured cross sections versus momentum. In the first two columns, no correction has been made for Monte Carlo acceptance.

Momentum (MeV/c)	g4	g6	g8	$g(\pi^0\pi^0)$
600	.1342	.4167	.2246	.0893
900	.1817	.4198	.1813	.1270
1050	.2093	.4239	.1641	.1492
1200	.1926	.4281	.1750	.1373
1350	.1768	.4278	.1893	.1208
1525	.1478	.4083	.2203	.0945
1642	.1342	.3937	.2410	.0810
1800	.1224	.3776	.2596	.0675
1940	.1193	.3760	.2557	.0628

Table 2: Branching ratios of $n\gamma$ to $(4+5+6+7+8)\gamma$; likewise for $\pi^0\pi^0$.